Optik - International Journal for Light and Electron Optics 242 (2021) 167150

Contents lists available at ScienceDirect

Optik

journal homepage: www.elsevier.com/locate/ijleo

Parameters identification of photovoltaic cells using improved version of the chaotic grey wolf optimizer

Jiawen Pan [a,b], Yang Gao [c], Qian Qian [a,b,*], Yong Feng [a,b], Yunfa Fu [a], Minghui sun [d], Farshid Sardari [e]

[a] Faculty of Information Engineering and Automation, Kunming University of Science and Technology, Kunming, Yunnan 650500, China
[b] Yunnan Key Laboratory of Computer Technology Applications, Kunming University of Science and Technology, Kunming, Yunnan 650500, China
[c] The University of Edinburgh, 57 George Square, Edinburgh EH8 9JU, UK
[d] College of Computer Science & Technology, Jilin University, Changchun 130012, China
[e] Department of Biosystems engineering, University of Mohaghegh Ardabili, Ardabil, Iran

ARTICLE INFO

Keywords:
Parameter identification
Photovoltaic cells
Single-diode model
Double-diode model
Three-diode model
ACGWO algorithm

ABSTRACT

Precise estimation of critical parameters of the photovoltaic models is a highly demanding task in modeling and simulation of the photovoltaic systems. In this paper, a new enhanced optimization method is proposed to estimate the unknown parameters of photovoltaic modules. The proposed adaptive chaotic grey wolf optimization (ACGWO) algorithm is employed to estimate the parameters of solar cells models for single-diode, double-diode, three-diode. The suggested optimization method is obtained by combining the adaptive grey wolf optimization (AGWO) and chaotic grey wolf optimization (CGWO) algorithms. Minimization of Root Mean Squared Error (RMSE) as employed as the common objective function. Besides, the results are compared with some well-known algorithms. The results of RMSE are compared with commonly used objective functions such as the sum of squared error (SSE) and Maximal Absolute Error (MAE). The efficiency of the ACGWO method is analyzed, and the results of the simulation report the lowest values for RMSE and confirm accuracy, robustness, and high convergence speed in comparison with some well-known optimization methods. According to the results, the proposed ACGWO could outperform four other methods competitive based on RMSE values, and the best values are reported for the ACGWO method.

1. Introduction

Nowadays, because of the increasing and instability of the prices of fossil fuels and problems originated from fossil fuels' pollutions and solid wastes, priorities have been given to renewable energy sources [1,2]. For instance, solar energy can be considered the most efficient alternative to fossil fuels and coal [3]. Recently, the use of solar energy worldwide is considered as the most promising renewable energy due to its significant advantages such as easily accessible in over the world, noise-free and simple fabrication methods. Besides, the price of solar cells considerably reduced during the years. In 1997, its cost was 76.67$/W and in 2017, it's cost was 0.37$/W. The reduction in the price of solar cells shows the utilization of solar panels increment in the future. The design of a more

* Corresponding author at: Faculty of Information Engineering and Automation, Kunming University of Science and Technology, Kunming, Yunnan 650500, China.
E-mail address: qianqian_yn@sina.com (Q. Qian).

https://doi.org/10.1016/j.ijleo.2021.167150
Received 4 October 2020; Received in revised form 6 April 2021; Accepted 11 April 2021
Available online 15 May 2021

efficient and accurate power generation system based on PV modules is an important consideration in this field. Obtaining precise variables of the PV panels according to their measured polarization curve is crucial in the performance assessment, optimum control, and operation of photovoltaic systems. In previous papers, most of the authors tried to identify the accurate parameters of PV cells for modeling the solar system behavior at various weather conditions [4–8]. Generally, the modeling of the PV systems is conducted based on the number of diodes. These scenarios are known as single-diode model (SDM), double-diode model (DDM), and three-diode model (TDM) [9].

In the first solar cell model, called SDM, only five unknown parameters are estimated; simplicity and accuracy are the main features of this model. The second method, called DDM, with seven unknown parameters, has higher accuracy compared to the first model. As a new model, the TDM is introduced with the highest accuracy, especially in low solar radiation conditions [10–14]. The increment of the accuracy increases the number of unknown parameters; subsequently, the complexity of parameter estimation increases.

To estimate the unknown parameters of PV, several methods have been employed in the literature. The popular scenarios for specifying the unknown parameters are the analytical methods, nonlinear optimization algorithms, and a combination of metaheuristics and analytical methods. In the analytical method, the suitable formulation techniques estimate the unknown variables based on datasheets or polarization curves [15–17]. Also, in the nonlinear optimization methods, the solution methods depend on empirically obtained data sets to identify the unknown parameters of solar cells [18–20]. Besides, in this scenario, some metaheuristic optimization algorithms are applied to solve the optimization problem. The third method combines metaheuristics and analytical methods as explained in Refs. [21,22]. Based on the previously discussed scenarios, the related developed works to estimate the PV unknown parameters are summarized in the following paragraphs.

A nonlinear least-squares optimization algorithm based on the Newton model modified with the Levenberg parameter was proposed for the identification of the five unknown PV parameters from the experimental data by Easwarakhanthan et al. [23]. The Genetic algorithm optimization to extract seven unknown variables of the PV panel was modeled by Ismail et al. [24]. The influence of solar radiation and ambient temperature was considered in fitness function assessment, and the accuracy and applicability of the proposed approach to be used as a valuable tool for PV modeling were clearly shown. To estimate the unknown parameters of the PV modules under the TDM model, Qais et al. [22] used the combined model of optimization and the analytical method by applying the sunflower optimization algorithm. The simulation results indicated an excellent agreement with the experimental data. Parameters extraction of the three-diode model for the multi-crystalline solar cell/module using the Moth-Flame optimization algorithm was carried out by Allam et al. [25]. The Bacterial Foraging algorithm was applied to identify the PV model parameters under normal and shading operation conditions [26].

Recently, to obtain the electrical parameters of SDPV and DDPV, metaheuristic optimizations are applied by minimizing an objective function. Accordingly, the root-mean-square error (RMSE) metric is employed mostly as the objective function, which is the root of the average differences between the experimental and simulated data [21]. Thus, many algorithms are utilized to minimize the mentioned objective function (RSME), such as particle swarm optimization (PSO) [27,28], artifice bee colony (ABC) hybridized with trusted region reflection algorithm [29], whale optimizer algorithm and its improved versions [30–33], Firefly optimization hybridized with pattern-search optimization [34], performance-guided JAYA algorithm (PGJAYA) [35], and improved JAYA (IJAYA) optimization algorithm [36].

Recently, researchers mostly used the TDPV model for precise modeling of PV. The three-diode model has nine unknown parameters, and the analysis of the equation is impossible due to a large number of nonlinear equations. Therefore, to identify these nine unknown parameters, the optimization algorithms are applied by minimizing the RMSE value as an objective function. In the recently published papers, several metaheuristic optimization approaches were used to specify nine unknown parameters of the PV module. For example, PSO [37], moth-flame optimizer [38], whale optimization algorithm [32], and Coyote optimization algorithm [39].

1.1. Main novelties and contributions

Based on the literature review and to the best of the author's knowledge, a significant attempt has been performed to characterize the unknown parameters of the PV cells in their optimal performance mode. This paper discusses the parameter identification of single-diode, double-diode, and three-diode PV models using the study case format and focuses on the optimization strategy based on its decision variables and objective analysis aspects. This paper proposed an adaptive chaotic version of the GWO algorithm achieving higher convergence speed and precision. Firstly, the chaotic algorithm is applied to the GWO algorithm to keep the population's diversity and offer an initial population with uniform distribution resulting in higher convergence speed. On the other hand, the high global exploration ability indicates a proper diversity of the population, and high location exploration results in higher accuracy. A nonlinear convergence factor is suggested in the proposed method to make a good balance between the global and local exploration capabilities. So, two enhancement factors are proposed in the ACGWO algorithm that can considerably enhance the convergence speed and the accuracy of results.

The suggested ACGWO algorithm is used here for a single-diode, double-diode, and three-diode models. Obtained results are completely authenticated by presented experimental data, and the proposed method is compared with other well-known optimization methods.

This rest of the work is structured as follow:

Section 2 presents the formulation of the single-diode, double-diode, and three-diode models. Section 3 discusses the proposed optimization method and its features for accurate characterization. The results of the proposed method along with comparisons with well-known algorithms and evaluation of the proposed method are represented in Section 4. Consequently, in Section 5, a comprehensive conclusion and future works are reported.

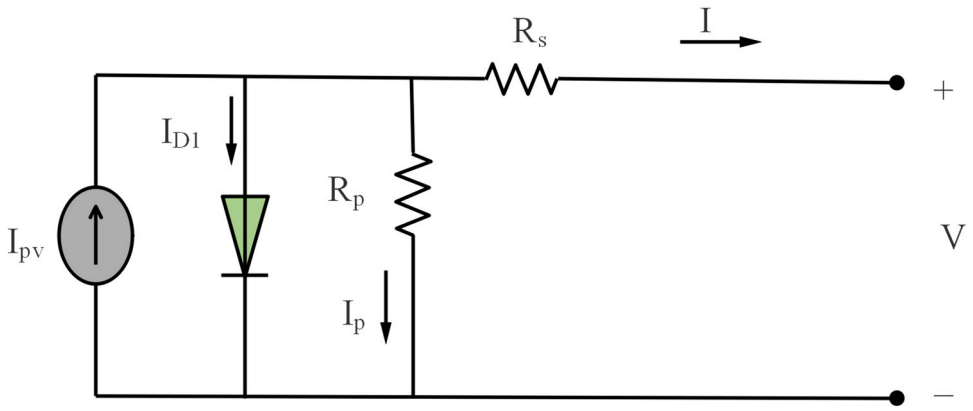

Fig. 1. Equivalent circuit of single-diode model.

2. Problem formulation

2.1. Solar cell models

There are different solar cell models, and these models all can express the current-voltage features of these cells. Between all these models, the single-diode, double-diode, and three-diode are the mostly-used models, chiefly for low irradiations. These three models assume that the output current of the solar cell (I) is calculated from the output voltage (V). These models are presented using an equivalent circuit in a determined set of operational conditions. The overall I−V profile for the cell is emulated as a continuous function. The relevant parameters to the PV operational conditions (e.g., temperature and irradiance) are assumed to be fixed. It's aimed to estimate the simplified inner characteristics (parameters) of the system, which relies on the selected model. Three considered models are expressed in the following subsections.

2.1.1. Single-diode model (SDM)

The equivalent circuit for this model is shown in Fig. 1. There is a current source (I_{PV}) in the SDM model presenting the photo-current in parallel with a diode, a resistance (R_P), and a series resistance (R_S). The resistance R_P considers the leakage current of P_N junction consisting of the partial short-circuit current path nearby the edges of the cell related to the impurity and non-ideality of the semiconductor. Also, R_S considers the effects of the contact surfaces of the silicon and electrodes, as well as the electrodes and the flowing current resistances [7]. The output current of SDM can be attained by [7]:

$$I = I_{PV} - I_{D1} - I_P \tag{1}$$

where I_{PV} and I_{D1} are the photons and diode currents, respectively. Also, I_P denotes the current passes through the shunt resistance. The diode current (I_{D1}) can be calculated based on the Shockley equation as follows [7]:

$$I_{D1} = I_{S1} \times \left[\exp\left(\frac{V + I \times R_S}{\eta_1 \times V_T}\right) - 1\right] \tag{2}$$

where I_{S1} is the reverse saturation current of diode, η_1 denotes the ideal coefficient of diode, I and V are the cell's output current and voltage, respectively. In this equation, I_P can be computed by [7]:

$$I_P = \frac{V + I \times R_S}{R_P} \tag{3}$$

where V_T is a constant value that is presented as [7]:

$$V_T = \frac{K_B.T}{q} \tag{4}$$

where K_B is the Boltzmann constant ($1.3806503 \times 10^{23} J/K$), T denotes the absolute temperature, and q indicates the basic electric charge ($1.60217646 \times 10^{-19} C$).

There are five unknown parameters, including I_{PV}, I_{S1}, η_1, R_P, and R_S in the single-diode model.

2.1.2. Double-diode model (DDM)

In the DDM model, another additional diode is shunted to the current source regarding the space charge recombination [40]. Fig. 2 depicts the DDM equivalent circuit. In the DDM model, the output current can be computed as [7]:

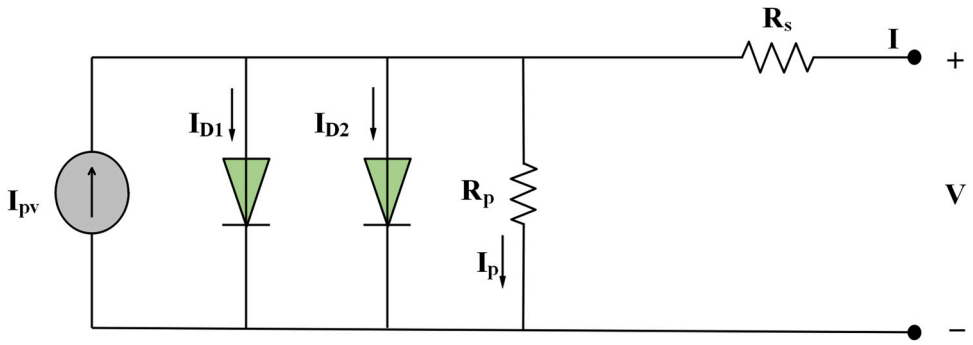

Fig. 2. Equivalent circuit of double-diode model.

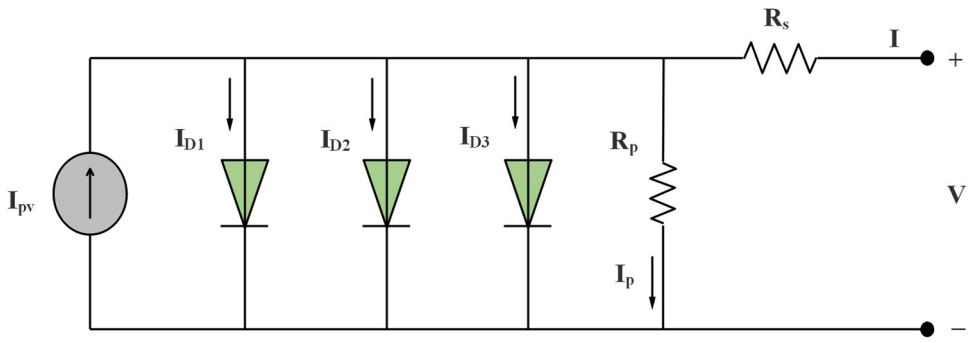

Fig. 3. Equivalent circuit of three-diode model.

$$I = I_{PV} - I_{D1} - I_{D2} - I_P \tag{5}$$

where I_{D2} denotes the current of the second diode, and it can be computed by [7]:

$$I_{D2} = I_{S2} \times \left[\exp\left(\frac{V + I \times R_S}{\eta_2 \times V_T}\right) - 1\right] \tag{6}$$

where I_{S2} and η_2 are the reverse saturation current and ideal coefficient of the second diode, respectively. There are seven unknown parameters (I_{PV}, I_{S1}, I_{S2}, η_1, η_2, R_P, and R_S) in DDM. This model has two additional parameters compared to SDM, which is needed to be extracted by the optimizer to obtain the vital status information of solar cells.

2.1.3. *Three-diode model (TDM)*

In the TDM scenario, the effect of the large leakage and recombination are remarked in the defect area. Hence, a third shunt diode is added to the equivalent circuit as depicted in Fig. 3.

Similar to two prior models, the output current can be computed by [7]:

$$I = I_{PV} - I_{D1} - I_{D2} - I_{D3} - I_P \tag{7}$$

where I_{D3} denotes the current of the third diode, and it's given as follows [7]:

$$I_{D3} = I_{S3} \times \left[\exp\left(\frac{V + I \times R_S}{\eta_3 \times V_T}\right) - 1\right] \tag{8}$$

where I_{S3} and η_3 are the reverse saturation current and ideality factor of the third diode, respectively.

In the present work, nine unknown parameters (I_{PV}, I_{S1}, I_{S2}, I_{S3} η_1, η_2, η_3, R_P, and R_S) are estimated for the TDM class achieving a model with higher precision.

2.2. *Parameter identification as an optimization*

Any optimization problem first aims to minimize an objective function. This function often has the concept of error and variance. An experimental dataset is utilized here to perform the optimization process [11,23]. Boundaries for parameters are employed combined with the previous models to obtain the best values for their parameters. Therefore, a classical bounded optimization is

Table 1
Lower and upper boundaries for SDM, DDM, and TDM scenarios.

Parameters	Lower bound	Upper bounds
$I_{PV}(A)$	0	1
$I_{S1}(\mu A)$	0	1
η_1	1	2
$R_p(\Omega)$	0	100
$R_S(\Omega)$	0	0.5
$I_{S2}(\mu A)$	0	1
η_2	1	2
$I_{S3}(\mu A)$	0	1
η_3	1	2

regarded without other constraints [7]:

$$\begin{aligned} &\text{Minimize f(x)} \\ &\text{Subject to :} \\ &a \le x \le b \end{aligned} \tag{9}$$

where $f(x)$ denotes the objective function, x is a vector of decision variables, and a and b are the lower and higher bounds of decision variables, respectively. The values of these bounds are listed in Table 1. As the objective function for these PV modules, the function of root mean square error (RMSE) is utilized here as expressed in Eq. (10) [7]:

$$RMSE = \sqrt{\frac{\sum_{i=1}^{N}[1 - I_i^{exp}]^2}{N}} \tag{10}$$

where I^{exp} indicates the experimental values of output current, N stands for the number of experimental data, and I is the calculated output currents using proposed models. Also, the simplified RMSE is defined as sum of squared error [7]:

$$SSE = \sum_{1}^{N} (I - I_i^{exp})^2 \tag{11}$$

RMSE and SSE behaviors are similar with exactly optimal solution and the values of SSE is always positive. To solve the optimal unknown parameters when the aim is minimizing the worst error and is not to reach average amount of variables, the Maximal Absolute Error is defined as [7]:

$$MAE = \|I - I^{exp}\|_{\infty} = \max(|I - I^{exp}|) \tag{12}$$

3. Proposed methodology

3.1. Grey wolf optimization method

Grey wolves prey on the smaller animals in nature, relying on their leadership hierarchy and hunting mechanism. This structure consists of four main layers for carrying out the hunting process. This management structure can be divided into four layers of α, β, δ, and ω. In the hunting process, the first three layers conduct the hunt and search. In addition, ω wolves should ensure safety/integrity and finally complete the predation. The α is responsible for guidance and decision making; β wolves are secondary wolves, and they assist α for collective acts (it's the best candidate for leadership); δ obey first two layers, while they dominate ω layer [41].

Grey wolves recognize and encircle prey, and the location of wolf (X, Y) is usually updated according to the position of prey (X′, Y′). In the population, the best one is named α, which is presented as the optimum point. The second and third optimal values are determined regarding the cost function as the suboptimal and final solutions (β and δ). The rest of particles will be categorized as ω wolves. In the D-dimensional search space, the number of grey wolves is assumed to be N, the number of iterations is expressed by t; the position vector of i^{th} grey wolf is computed by below relations [41]:

$$\vec{X}_{id}(t+1) = \vec{X}_{pd}(t) - \vec{A}_{id} \cdot \vec{D}_{id} \tag{13}$$

$$\vec{D}_{id} = \left| \vec{C}_{id} \cdot \vec{X}_{pd}(t) - \vec{X}_{id}(t) \right| \tag{14}$$

where $\vec{X}_i$ is the position vector of a grey wolf, $\vec{X}_p$ is the position vector of the prey, $\vec{C}_{id}$ and $\vec{A}_{id}$ are coefficient vectors and computed as follows [41]:

$$\vec{C}_{id} = 2\vec{r}_2 \tag{15}$$

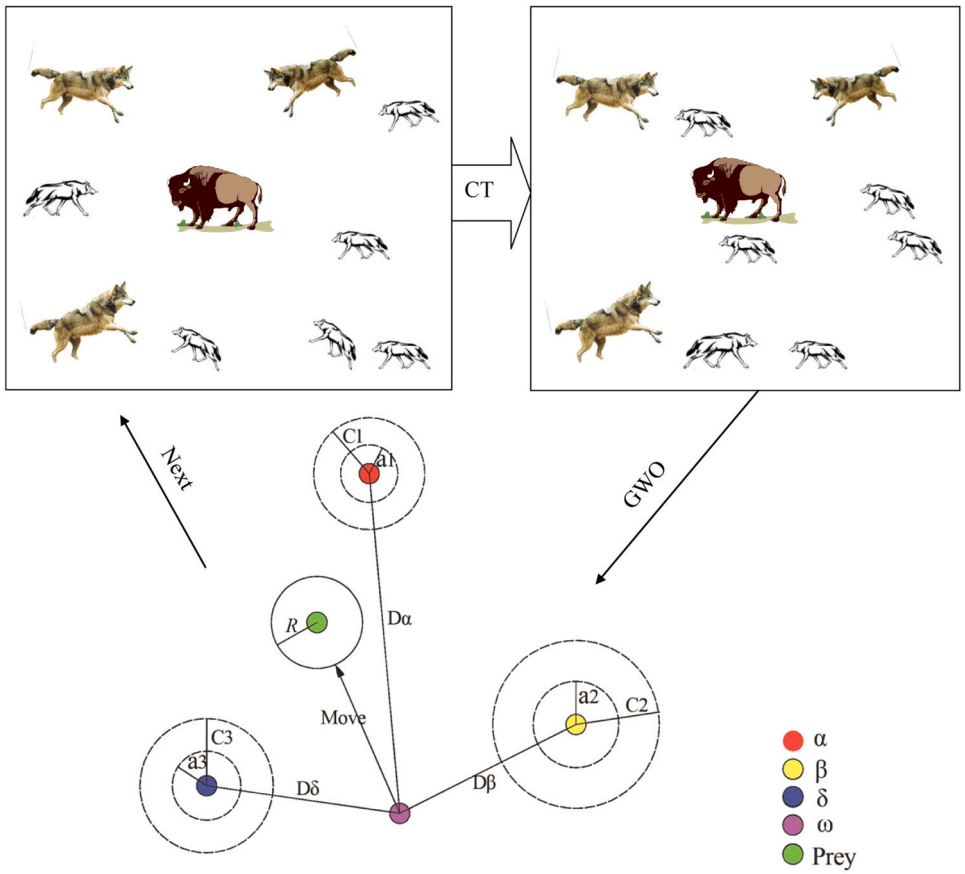

Fig. 4. Schematic diagram of CGWO method.

$$\vec{A}_{id} = 2\vec{a}.\vec{r}_1 - \vec{a} \tag{16}$$

where $\vec{a}$ denotes the convergence factor and the components of $\vec{a}$ are linearly decreased from 2 to 0 over the course of iterations. Also, $\vec{r}_1$ and $\vec{r}_2$ are random vectors in the range of [0,1]. So, the prey's location vector is computed by:

$$\left\{ \vec{X}_{ijd}(t+1) = \vec{X}_{jd}(t) - \vec{A}_{id} \cdot \vec{D}_{ijd}\vec{X}_{id}(t+1) = \frac{\sum_j \vec{X}_{ijd}(t+1)}{3} \right\}, \quad j = \alpha, \quad \beta, \quad \delta \tag{17}$$

After each iteration, the three best solutions are assigned to α, β, and δ. Locations of other wolves will be updated regarding the locations of these three best solutions. In fact, these three best solutions estimate the prey's location, and other wolves update their locations randomly around the prey. The prey's location is the final optimum point that will be obtained after several iterative steps.

3.2. Initializing based on the chaotic algorithm

The chaotic algorithm is proposed and applied to the GWO optimization method achieving higher convergence speed. This algorithm can keep the population's diversity, and provide an initial population with uniform distribution. Firstly, chaos parameters are linearly mapped to the exploration domain, and the chaos transform is employed for exploration aims. Trapping in local optimal points can be avoided by the chaos randomness and ergodicity in the exploration procedure. So, the disadvantages of the basic GWO algorithm can be tackled by this improvement. The logistic mapping is selected here with proper uniformity and ergodicity, and map relation can be presented by:

$$x_{n+1} = \mu x_n[1 - x_n] \tag{18}$$

The population is in a chaotic state when $\mu = 4$, and its output has a random value in the range of [0,1], which can traverse each number of interval [0,1] without any repetition. This mapping method, with simple structure and proper traversal uniformity, has a

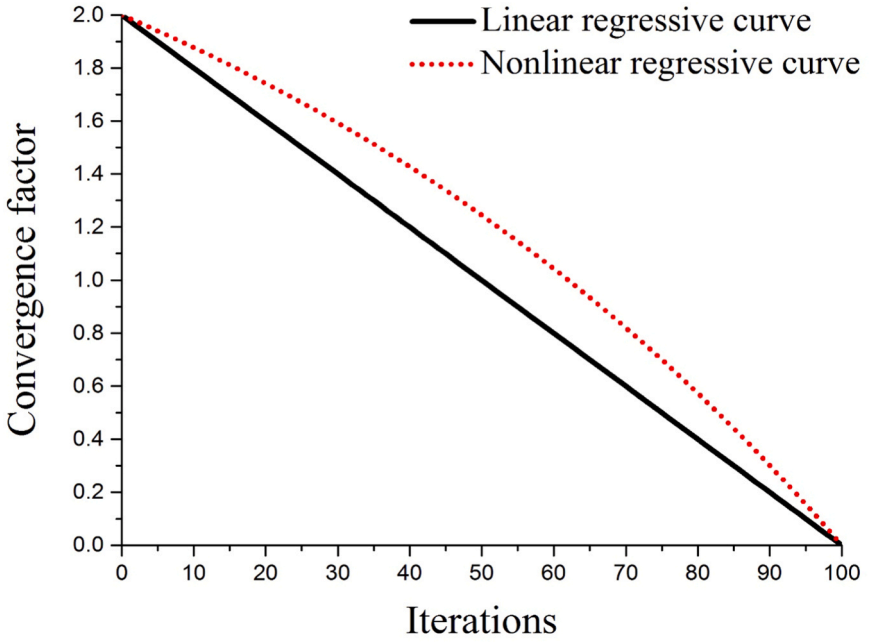

Fig. 5. The nonlinear convergence factor a introduced in AGWO algorithm.

high speed that makes the cost function to converge easier. The Chaotic GWO (CGWO) process is clearly depicted in Fig. 4.

3.3. Enhanced convergence factor

The coordinated problem between global and local exploration abilities is a common problem in the group of artificial methods. The high global exploration capability denotes a good population's diversity, while the high location exploration ability indicates the high accuracy of results. So, it's important to make coordination between these two exploration abilities in the GWO optimization method. In the original GWO method, the convergence factor (a) reduces linearly by the growth of the iterations number. While the method does not converge linearly in the optimization process. In other words, the convergence factor is not able to fully reflect the real optimization procedure.

In this paper, a nonlinear convergence factor is proposed for keeping the balance between the global and local exploration abilities as:

$$a = 2 - 2 \times \left[\left[\frac{1}{e-1} \right] \times \left[\exp\left(\frac{t}{m}\right) - 1 \right] \right] \tag{19}$$

where e is the number of natural logarithms, t is the real number of current iterative steps, and m denotes the maximum iteration number.

Regarding Fig. 5, a nonlinearly reduces by the growth of the iterations number in the range of 2–0. Firstly, the reduction rate of the convergence factor is decreased for finding the optimum global point in the lowest possible time. Then, the reduction rate is growing for precisely finding the local optimum point. Thus, the nonlinear convergence factor can make a proper trade-off between the global and local exploration abilities to enhance the convergence stability. This improved convergence factor resulted in an improved version of GWO (AGWO).

Finally, a novel optimization method is obtained through a combination of AGWO and CGWO algorithms as the ACGWO algorithm. The optimization process of the ACGWO optimization method is comprehensively illustrated in Fig. 6. Adjustable parameters of the algorithm should be set at the first time. Then, the fitness values of particles are computed and saved. From these fitness values, three best values are saved as α,β, and δ. Afterward, locations of ω particles are updated as well as the chaotic sequence. In the next step, the iteration's number and convergence factor are updated for computing the value of the enhanced $\vec{a}$. Also, other parameters ($\vec{r_1}$, $\vec{r_2}$, $\vec{a}$, $\vec{C_{id}}$, $\vec{A_{id}}$, and x_n) are updated. At last, the final optimum point (α) will be determined as the best solution.

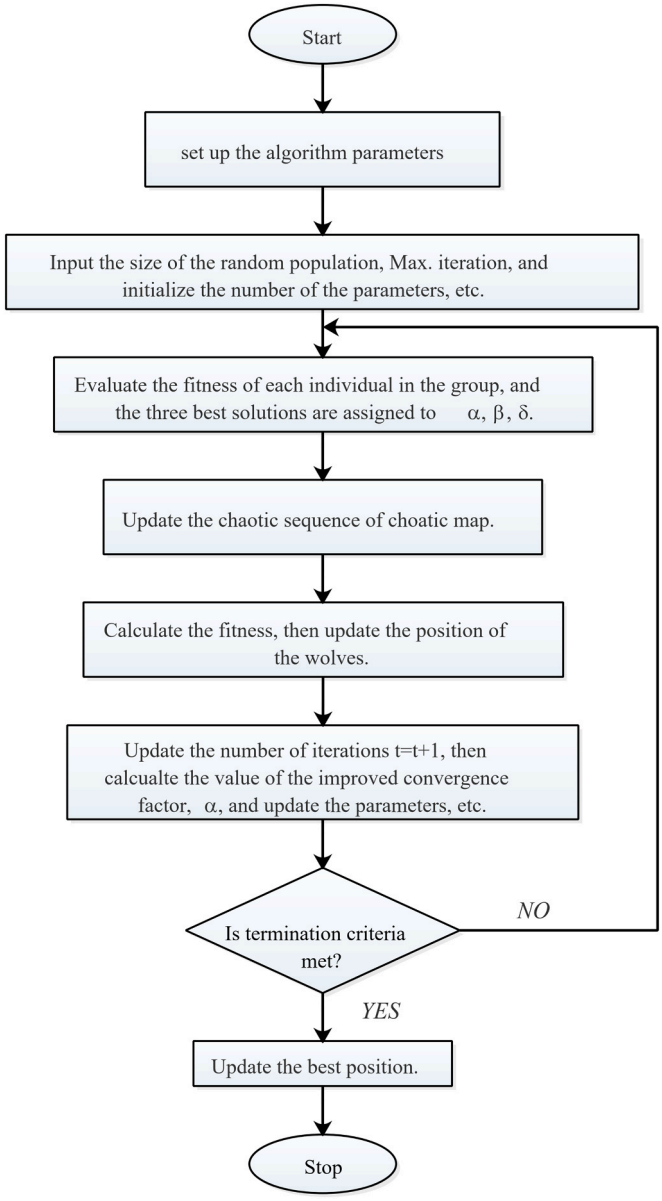

Fig. 6. Flowchart of the proposed ACGWO algorit.

4. Results and discussion

4.1. Operation condition

Several experiments are employed in this study to investigate the operations of the new variant. The employed PV cell is the 57mm diameter silicon solar cell that is known as commercial RT.C. France silicon solar cell with an irradiance of 1000W/m^2 and a temperature of 33 °C [23]. Based on the ACGWO optimization algorithm and RSME as the objective function, the estimated results for unknown parameters of PV cells are obtained in which the identified parameters are according to SDM, DDM, and TDM. All of the intended models are run by a 3.7 GHz Intel(R) Core™ computer with 8 GB RAM with stop criteria of 5000*s*. Also, the model is implemented and executed in Matlab-2017a.

4.2. Comparative performance of the proposed method

To illustrate the effectiveness of the proposed hybrid algorithm, ACGWO is compared with other algorithms. The comparative

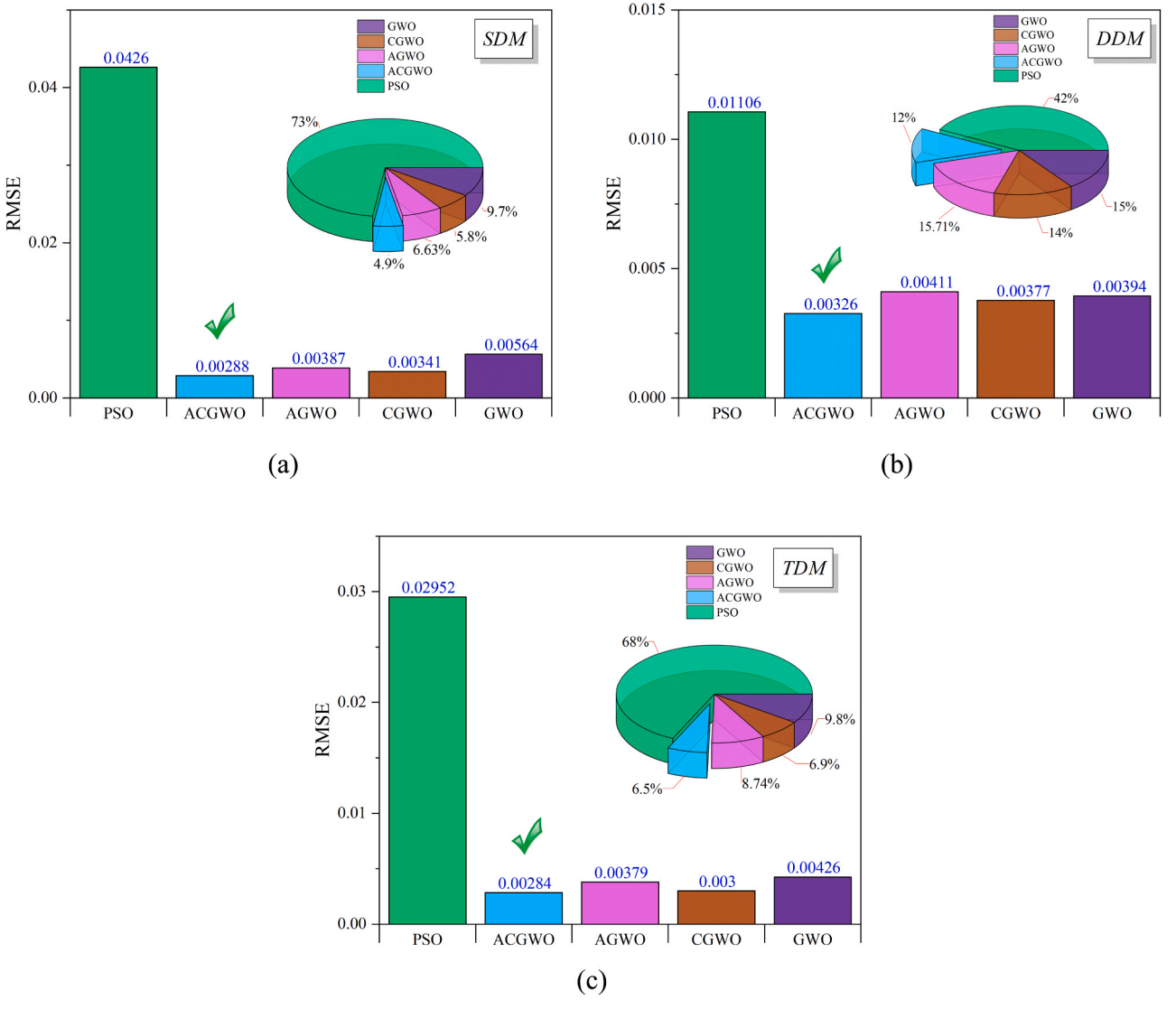

Fig. 7. Obtained RMSE value as objective function for proposed and other comparative methods under various scenarios of SDM, DDM, and TDM.

Table 2
Results of optimization based on the proposed method for SDM, DDM, and SDM scenarios.

Parameter	GWO	CGWO	AGWO	ACGWO	PSO
Single-diode model (SDM)					
I_{PV} (A)	0.765456	0.758561	0.761199	0.760632	0.813115
I_{S1} (μA)	1.38×10^{-7}	1.37×10^{-7}	1.39×10^{-7}	1.38×10^{-7}	7.58×10^{-7}
η_1	1.4	1.4	1.4	1.4	1.564258
$R_P(\Omega)$	50	50	63.27924	50	89.13647
$R_S(\Omega)$	0.040944	0.039406	0.040918	0.039072	0.048353
RMSE	0.00564	0.003411	0.003871	***0.002877***	0.042601
MAE	0.015221	0.011399	0.010927	***0.006236***	0.057044
SSE	0.000827	0.000303	0.00039	***0.000215***	0.047186
Double-diode model (DDM)					
I_{PV} (A)	0.756905	0.756674	0.761924	0.758538	0.746191
I_{S1} (μA)	8.23×10^{-8}	1.28×10^{-7}	8.9×10^{-8}	1.38×10^{-7}	3.6×10^{-7}
η_1	1.9	1.4	1.713794	1.4	1.503333
$R_P(\Omega)$	82.58175	50	87.17771	80.64198	75.99742
$R_S(\Omega)$	0.036187	0.03944	0.03991	0.040189	0.031874
I_{S2} (μA)	2.38×10^{-7}	1×10^{-8}	1.34×10^{-7}	1.88×10^{-7}	4.78×10^{-7}
η_2	1.451407	1.4	1.4	2	1.84751
RMSE	0.003943	0.00377	0.004106	***0.003263***	0.01106
MAE	0.010598	0.007577	0.009711	***0.005303***	0.015422
SSE	0.000404	0.000438	0.000369	***0.000277***	0.00318
Three-diode model (TDM)					
I_{PV} (A)	0.764767	0.757032	0.760787	0.760638	0.733044
I_{S1} (μA)	3.6×10^{-8}	1.34×10^{-7}	1.29×10^{-7}	1.55×10^{-7}	3.86×10^{-7}
η_1	1.4	1.4	1.4	1.9	1.770531
$R_P(\Omega)$	60	82.40509	78.62991	75.6424	83.09683
$R_S(\Omega)$	0.033259	0.04	0.038668	0.039766	0.033438
I_{S2}(μA)	6.55×10^{-7}	1.72×10^{-8}	9.53×10^{-7}	1.46×10^{-7}	8.19×10^{-7}
η_2	1.6	1.6	2	1.6	1.682576
I_{S3}(μA)	0.000001	1.97×10^{-9}	1×10^{-9}	1.14×10^{-7}	6.08×10^{-7}
η_3	2	1.4	1.4	1.4	1.656914
RMSE	0.004256	0.002996	0.003791	***0.002838***	0.029519
MAE	0.009125	0.015499	***0.006732***	0.007195	0.043873
SSE	0.000471	0.000374	0.000233	***0.00021***	0.022656

metaheuristic algorithms are PSO, CGWO, AGWO, and GWO. For a fair comparison, all of the algorithms use the same maximum number of function evaluations of 5,000 in every run. To minimize the statistical error, algorithms are independently run 30 times. Minimizing RMSE as an objective function is the base aim of accurate simulation of PV modules in the current paper. Experimentally obtained results are briefly presented in Fig. 7 for SDM, DDM, and TDM. Regarding the obtained results, the proposed ACGWO could outperform four other methods based on RMSE values, and the best values are reported for this method. According to Fig. 7a-c, among the involved four algorithms in terms of accumulated RMSE value, the proposed optimization method has the lowest percentages, 4.9%, 12%, and 2.5%, for SDM, DDM, and TDM, respectively. In addition, for the single-diode model, double-diode, and three-diode model, the comparison results, including the estimated parameters and RMSE, MAE, and SSE, are represented in Table 2. As shown in this table, the ACGWO method provides the least RMSE of 0.002877, 0.003263, and 0.002838 for SDM, DDM, and TDM, respectively, compared to other comparative algorithms. Besides, similar to RMSE, the SSE metric has the lowest values for the proposed ACGWO method in SDM, DDM, and TDM, about 0.000215, 0.000277, and 0.00021, respectively. In the case of MAE criteria, the proposed method has the lowest values in SDM and DDM scenarios, and for the TDM, AGWO has the lowest value, about 0.006732, while the computed value for the proposed ACGWO is 0.007195.

The histogram of the relative errors is also plotted and shown in Fig. 8 to determine the frequency of each error value. The higher frequency of the error values of zero or close to zero can be a piece of good evidence for a more accurate parameter identification. Fig. 8a shows the histogram for the total current in different models for the various comparative optimization algorithms. As demonstrated in Fig. 8a, for the case of ACGWO algorithm, the highest number of cases is found for situations where there is minor error (the Zero Error line), with the histogram similar to the Gaussian bell curve; this shows that the ACGWO algorithm concentrates the highest number of cases in situations with lower error.

Fig. 8a shows the histogram for the total power in different models for the various comparative optimization algorithms. As shown in Fig. 8b, for the case of ACGWO algorithm, the highest number of cases is found for situations where there is no error, with the histogram similar to the Gaussian bell curve; this shows that the ACGWO algorithm concentrates the highest number of cases in

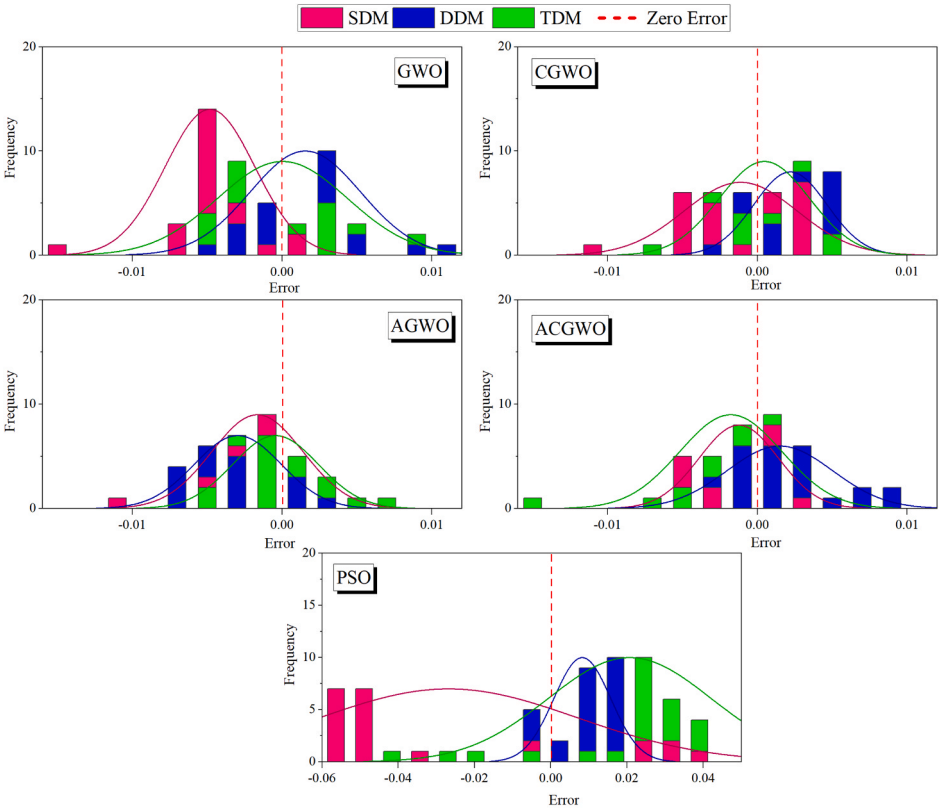

(a)

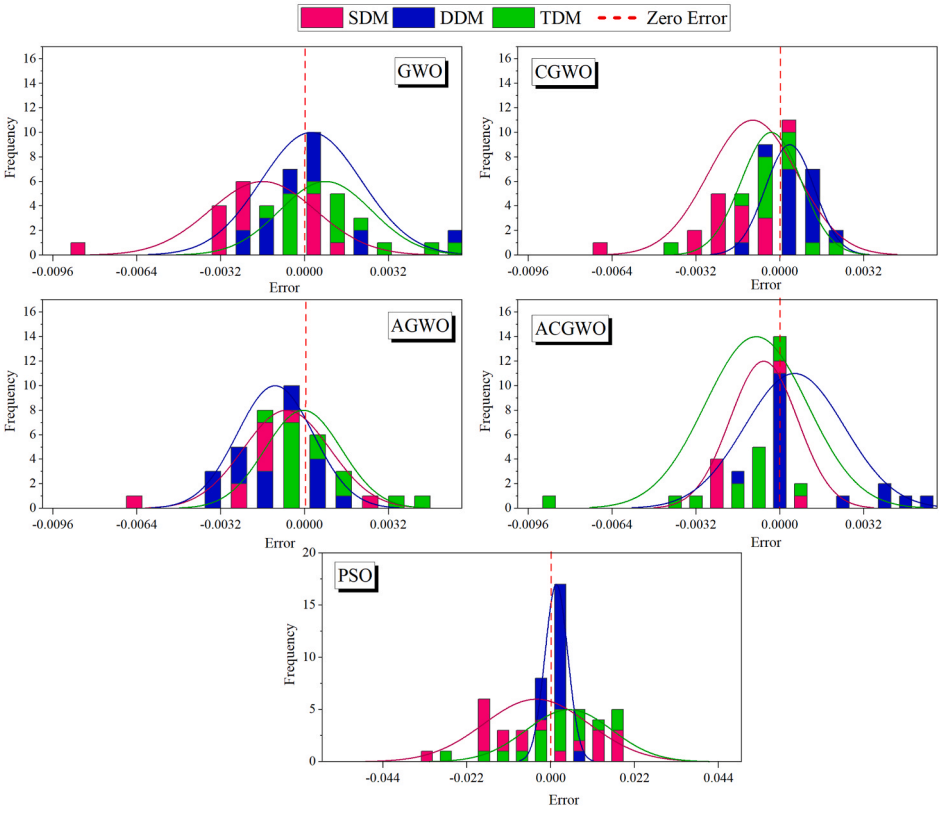

(b)

(caption on next page)

Fig. 8. Error histogram graph for the a) total current, and b) total power under various scenarios of SDM, DDM, and TDM.

situations with lower error.

4.3. Optimization results of the proposed method

To show the accuracy of the proposed method, the obtained data by the simulation for single, double, and three diode models is compared with experimental data in Figs. 9 and 10. Based on Fig. 9, the behavior of current with the variation of voltage for experimental and simulated data is illustrated. Also, Fig. 10 is plotted for the power-voltage variations, and similar to Fig. 9, the PV module is simulated for all of the three models. It is clearly observed that the obtained data by ACGWO are highly in accordance with the experimental data over the entire voltage interval. The absolute errors of current and power in contrast to the voltage changes between measured and simulated current and also measured and simulated power using the proposed method can be presented by Fig. 11 (a) and (b). What stands from these figures is that the suggested method has good agreement with the laboratory data under various simulation models (SDM, DDM, and TDM), and all of the errors for $I-V$ and $P-V$ curves are lower than 0.00522 and 0.003, respectively, a deeply lower absolute error. So, the results of the figures show that the computed data are in highly match with the experimental data over the whole voltages.

4.4. The convergence of the proposed method

The convergence curves of the proposed ACGWO method along with the other comparative algorithms (GWO, CGWO, AGWO, and PSO) for various models of the PV (SDM, DDM, and TDM) are illustrated in Fig. 12a-c. For the single-diode model, ACGWO converges to the optimal model at RMSE of 0.00288 and function evaluation of 562*s*. For the double-diode model, the converges speed of the ACGWO method is 4162*s*, with the lowest RMSE value of 0.00326. Similar to the DDM, the lowest convergence curve at the range of intended fitness evaluation is belong to the proposed ACGWO method with RMSE of 0.00284 and fitness evaluation of 4791*s*. According to these results, it can be pointed out clearly that the proposed ACGWO algorithm has very competitive efficiency due to its accuracy and reliability for solving the variables estimation problems of various PV models.

5. Conclusions

In this study, a new optimization algorithm is proposed for effectively identifying the unknown parameters of single-diode, double-diode, and three-diode models of the solar cell model and photovoltaic modules. The proposed method is a combination of AGWO and CGWO algorithms as an improved chaotic grey wolf optimization (ACGWO) algorithm that is recognized as a method with higher efficiency, greater robustness, and reasonable convergence rates. The proposed method is for the first time designed for accurately estimation of parameters on photovoltaic models. The modeling is performed for a commercial RT.C. France silicon solar cell, and well agreement between obtained values of unknown parameters by the ACGWO method and experimental data is obvious. Besides, the results are compared with some well-known algorithms. According to the competitive and statistical experimental results, several conclusions can be given as follow:

- According to the results, the proposed ACGWO could outperform four other methods (e.g., PSO, CGWO, AGWO, and GWO) based on RMSE values, and the best values are reported for the ACGWO method.
- The ACGWO method revealed the lowest RMSE of 0.002877, 0.003263, and 0.002838 for SDM, DDM, and TDM, respectively.
- The SSE metric has the lowest values for the proposed ACGWO method in SDM, DDM, and TDM, about 0.000215, 0.000277, and 0.00021, respectively.
- The ACGWO algorithm concentrates the highest number of cases in situations with lower error.
- According to the convergence speed, it can be pointed out that the proposed ACGWO algorithm has very competitive efficiency due to its speed, accuracy and reliability.

The future research directions mainly include the following aspects. First, to further improve study trustworthiness, we need to use the latest algorithm improved as a comparison algorithm. Second, the parameter setting of ACGWO is a complicated and vital problem. Generally, the determination of parameters is usually based on experience and lacks scientific theory support. Therefore, in the future study, we need to analyze the parameter values from the theoretical point of view and establish a solid theoretical basis for parameter adjustment. Besides, the proposed ACGWO can be developed to solve discrete optimization problems in the energy field, such as solid oxide fuel cells.

Declaration of Competing Interest

The authors declare that they have no known competing financial interests or personal relationships that could have appeared to influence the work reported in this paper.

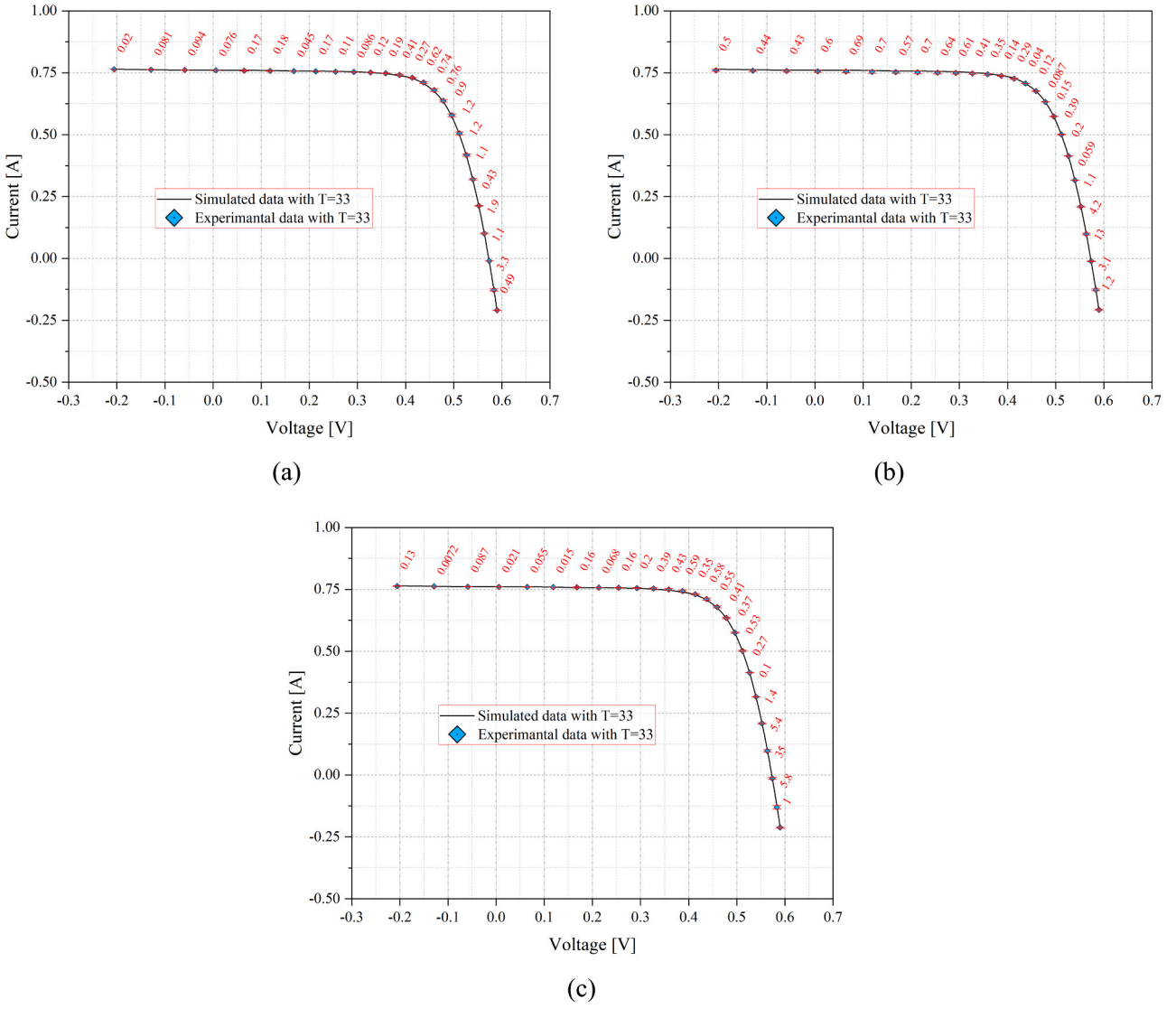

Fig. 9. Simulated $I-V$ characteristics of considered PV module for (a) single-diode model, (b) double-diode model, and (c) three-diode model.

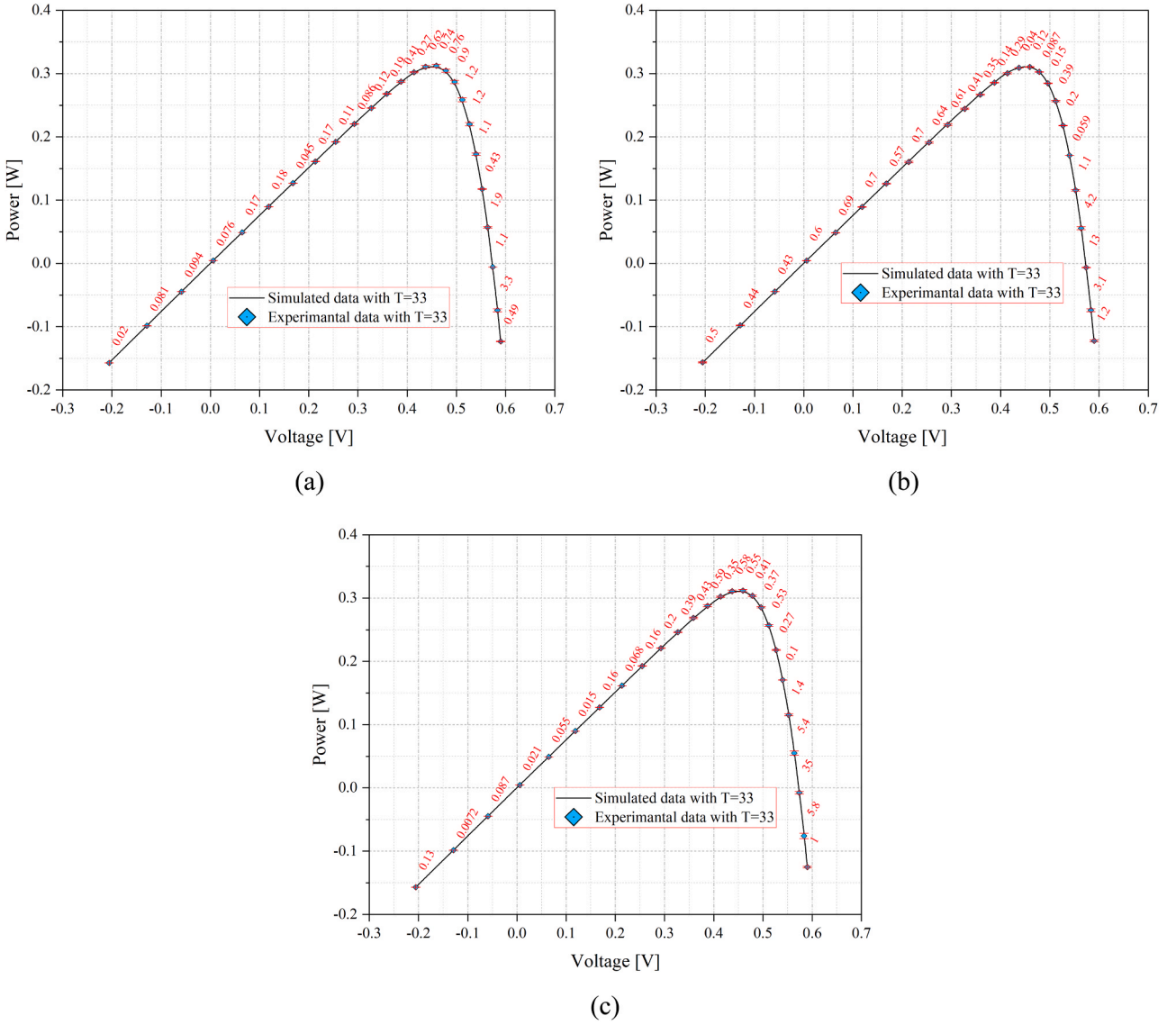

Fig. 10. Simulated $P-V$ characteristics of considered PV module for (a) single-diode model, (b) double-diode model, and (c) three-diode model.

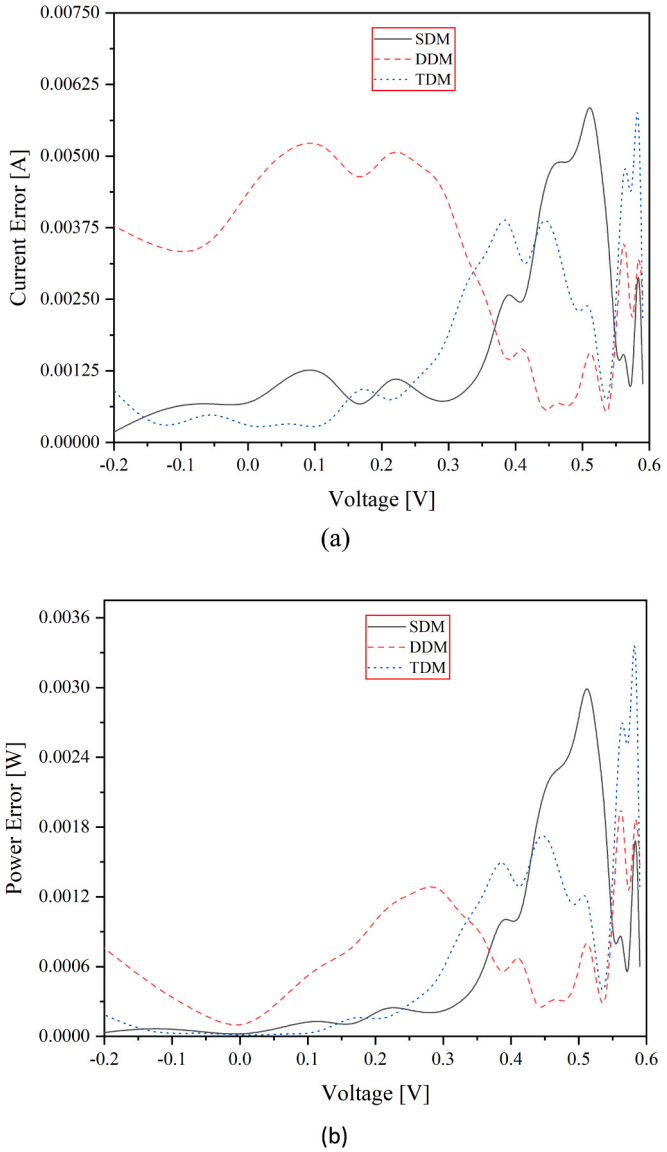

Fig. 11. Errors of obtained data based on proposed method under various number of diode for (a) current, and (b) power.

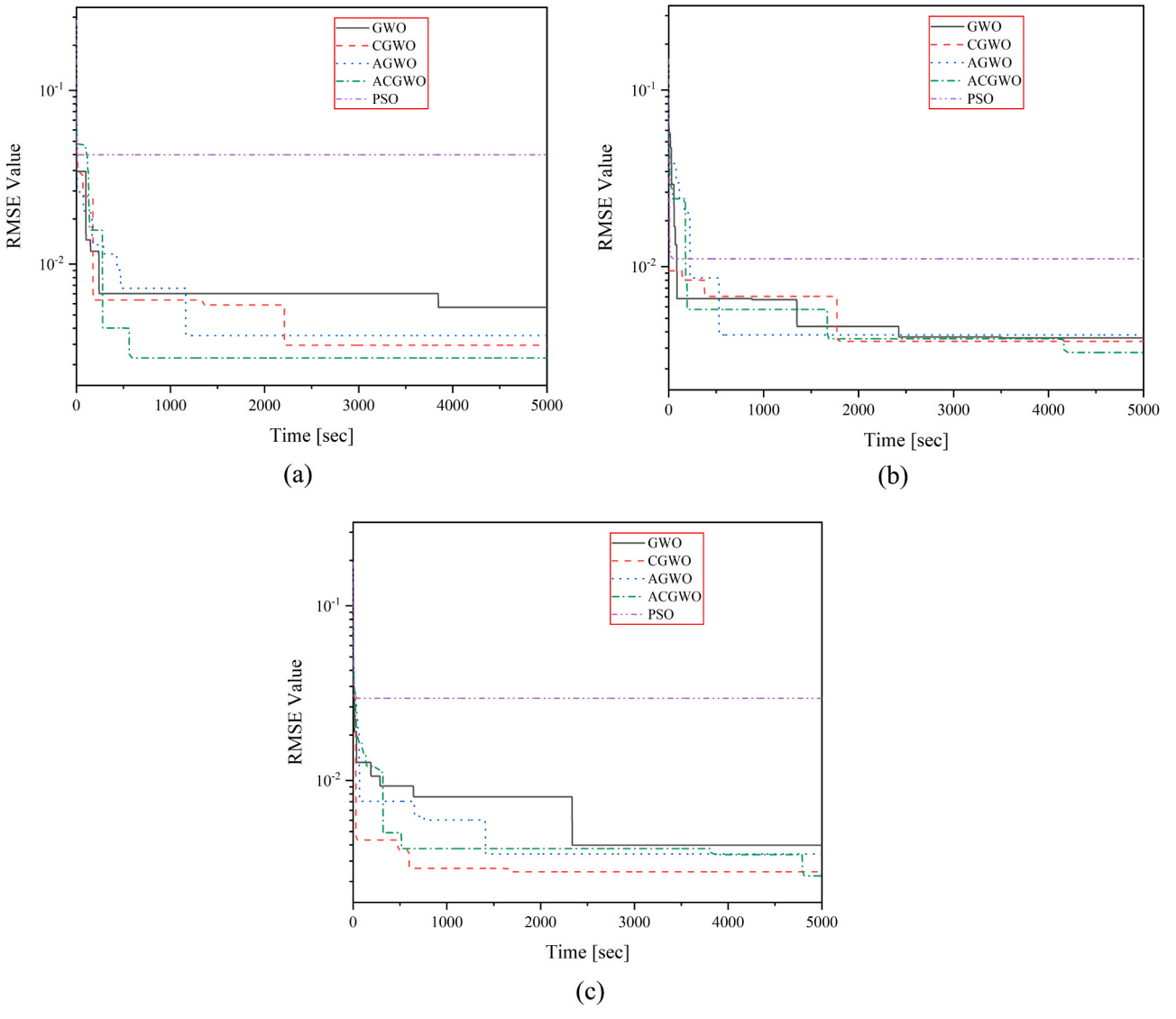

Fig. 12. Convergence curves of proposed method along with other comparative algorithms for various number of diode (a) single-diode model, (b) double-diode model, and (c) three-diode model.

Acknowledgments

This work was supported by National Science Foundation of China (Grant nos. 32060193, 81470084, 61463024).

References

[1] F. Hamrang, A. Shokri, S.M.S. Mahmoudi, B. Ehghaghi, Performance Analysis of a New Electricity and Freshwater Production System Based on an Integrated Gasification Combined Cycle and Multi- Effect Desalination, (2020). https://doi.org/10.3390/su12197996.
[2] S. Ahmadi, H. Ghaebi, A. Shokri, A comprehensive thermodynamic analysis of a novel CHP system based on SOFC and APC cycles, Energy 186 (2019), 115899, https://doi.org/10.1016/j.energy.2019.115899.
[3] B.M. Ziapour, M. Saadat, V. Palideh, S. Afzal, Power generation enhancement in a salinity-gradient solar pond power plant using thermoelectric generator, Energy Convers. Manag. 136 (2017) 283–293.
[4] J. Song, B. Sobhani, Energy and exergy performance of an integrated desiccant cooling system with photovoltaic/thermal using phase change material and maisotsenko cooler, J. Energy Storage 32 (2020), 101698.
[5] H. Shayeghi, B. Sobhani, E. Shahryari, A. Akbarimajd, Optimal neuro-fuzzy based islanding detection method for Distributed Generation, Neurocomputing 177 (2016) 478–488.
[6] N. Wang, D. Wang, Y. Xing, L. Shao, S. Afzal, Application of co-evolution RNA genetic algorithm for obtaining optimal parameters of SOFC model, Renew. Energy 150 (2020) 221–233.
[7] R. Chenouard, R.A. El-Sehiemy, An interval branch and bound global optimization algorithm for parameter estimation of three photovoltaic models, Energy Convers. Manag. 205 (2020), 112400.
[8] B. Amrouche, A. Guessoum, M. Belhamel, A simple behavioural model for solar module electric characteristics based on the first order system step response for MPPT study and comparison, Appl. Energy 91 (2012) 395–404.
[9] H. Chen, S. Jiao, M. Wang, A.A. Heidari, X. Zhao, Parameters identification of photovoltaic cells and modules using diversification-enriched Harris hawks optimization with chaotic drifts, J. Clean. Prod. 244 (2020), 118778.
[10] K. Nishioka, N. Sakitani, Y. Uraoka, T. Fuyuki, Analysis of multicrystalline silicon solar cells by modified 3-diode equivalent circuit model taking leakage current through periphery into consideration, Sol. Energy Mater. Sol. Cells 91 (2007) 1222–1227.
[11] A. Kassis, M. Saad, Analysis of multi-crystalline silicon solar cells at low illumination levels using a modified two-diode model, Sol. Energy Mater. Sol. Cells 94 (2010) 2108–2112.
[12] D.S.H. Chan, J.C.H. Phang, Analytical methods for the extraction of solar-cell single-and double-diode model parameters from IV characteristics, IEEE Trans. Electron Devices 34 (1987) 286–293.
[13] K. Ishaque, Z. Salam, H. Taheri, Modeling and simulation of photovoltaic (PV) system during partial shading based on a two-diode model, Simul. Model. Pract. Theory 19 (2011) 1613–1626.
[14] A.A. Elbaset, H. Ali, M. Abd-El Sattar, Novel seven-parameter model for photovoltaic modules, Sol. Energy Mater. Sol. Cells 130 (2014) 442–455.
[15] D.S.H. Chan, J.R. Phillips, J.C.H. Phang, A comparative study of extraction methods for solar cell model parameters, Solid. State Electron. 29 (1986) 329–337.
[16] A. Jain, A. Kapoor, A new approach to study organic solar cell using Lambert W-function, Sol. Energy Mater. Sol. Cells 86 (2005) 197–205.
[17] H. Saleem, S. Karmalkar, An analytical method to extract the physical parameters of a solar cell from four points on the illuminated $ J {-} V $ curve, IEEE Electron Device Lett. 30 (2009) 349–352.
[18] M.R. AlRashidi, M.F. AlHajri, K.M. El-Naggar, A.K. Al-Othman, A new estimation approach for determining the I–V characteristics of solar cells, Sol. Energy 85 (2011) 1543–1550.
[19] H. Wei, J. Cong, X. Lingyun, S. Deyun, Extracting solar cell model parameters based on chaos particle swarm algorithm, in: 2011 Int. Conf. Electr. Inf. Control Eng., IEEE, 2011: pp. 398–402.
[20] K.M. El-Naggar, M.R. AlRashidi, M.F. AlHajri, A.K. Al-Othman, Simulated annealing algorithm for photovoltaic parameters identification, Sol. Energy 86 (2012) 266–274.
[21] A.R. Jordehi, Parameter estimation of solar photovoltaic (PV) cells: a review, Renew. Sustain. Energy Rev. 61 (2016) 354–371.
[22] M.H. Qais, H.M. Hasanien, S. Alghuwainem, Identification of electrical parameters for three-diode photovoltaic model using analytical and sunflower optimization algorithm, Appl. Energy 250 (2019) 109–117.
[23] T. Easwarakhanthan, J. Bottin, I. Bouhouch, C. Boutrit, Nonlinear minimization algorithm for determining the solar cell parameters with microcomputers, Int. J. Sol. Energy 4 (1986) 1–12.
[24] M.S. Ismail, M. Moghavvemi, T.M.I. Mahlia, Characterization of PV panel and global optimization of its model parameters using genetic algorithm, Energy Convers. Manag. 73 (2013) 10–25.
[25] D. Allam, D.A. Yousri, M.B. Eteiba, Parameters extraction of the three diode model for the multi-crystalline solar cell/module using Moth-Flame Optimization Algorithm, Energy Convers. Manag. 123 (2016) 535–548.
[26] M.A. Awadallah, Variations of the bacterial foraging algorithm for the extraction of PV module parameters from nameplate data, Energy Convers. Manag. 113 (2016) 312–320.
[27] J. Liang, S. Ge, B. Qu, K. Yu, F. Liu, H. Yang, P. Wei, Z. Li, Classified perturbation mutation based particle swarm optimization algorithm for parameters extraction of photovoltaic models, Energy Convers. Manag. 203 (2020), 112138.
[28] S.M. Ebrahimi, E. Salahshour, M. Malekzadeh, F. Gordillo, Parameters identification of PV solar cells and modules using flexible particle swarm optimization algorithm, Energy 179 (2019) 358–372.
[29] L. Wu, Z. Chen, C. Long, S. Cheng, P. Lin, Y. Chen, H. Chen, Parameter extraction of photovoltaic models from measured IV characteristics curves using a hybrid trust-region reflective algorithm, Appl. Energy 232 (2018) 36–53.
[30] D. Oliva, M. Abd El Aziz, A.E. Hassanien, Parameter estimation of photovoltaic cells using an improved chaotic whale optimization algorithm, Appl. Energy 200 (2017) 141–154.
[31] O.S. Elazab, H.M. Hasanien, M.A. Elgendy, A.M. Abdeen, Parameters estimation of single-and multiple-diode photovoltaic model using whale optimisation algorithm, IET Renew. Power Gener. 12 (2018) 1755–1761.
[32] M. Abd Elaziz, D. Oliva, Parameter estimation of solar cells diode models by an improved opposition-based whale optimization algorithm, Energy Convers. Manag. 171 (2018) 1843–1859.
[33] G. Xiong, J. Zhang, D. Shi, Y. He, Parameter extraction of solar photovoltaic models using an improved whale optimization algorithm, Energy Convers. Manag. 174 (2018) 388–405.
[34] A.M. Beigi, A. Maroosi, Parameter identification for solar cells and module using a Hybrid Firefly and Pattern Search Algorithms, Sol. Energy 171 (2018) 435–446.
[35] K. Yu, B. Qu, C. Yue, S. Ge, X. Chen, J. Liang, A performance-guided JAYA algorithm for parameters identification of photovoltaic cell and module, Appl. Energy 237 (2019) 241–257.
[36] K. Yu, J.J. Liang, B.Y. Qu, X. Chen, H. Wang, Parameters identification of photovoltaic models using an improved JAYA optimization algorithm, Energy Convers. Manag. 150 (2017) 742–753.
[37] V. Khanna, B.K. Das, D. Bisht, P.K. Singh, A three diode model for industrial solar cells and estimation of solar cell parameters using PSO algorithm, Renew. Energy 78 (2015) 105–113.
[38] A. Fathy, M. Abd Elaziz, E.T. Sayed, A.G. Olabi, H. Rezk, Optimal parameter identification of triple-junction photovoltaic panel based on enhanced moth search algorithm, Energy 188 (2019), 116025.

[39] M.H. Qais, H.M. Hasanien, S. Alghuwainem, A.S. Nouh, Coyote optimization algorithm for parameters extraction of three-diode photovoltaic models of photovoltaic modules, Energy 187 (2019), 116001.
[40] A. Askarzadeh, A. Rezazadeh, Parameter identification for solar cell models using harmony search-based algorithms, Sol. Energy 86 (2012) 3241–3249.
[41] S. Mirjalili, S.M. Mirjalili, A. Lewis, Grey wolf optimizer, Adv. Eng. Softw. 69 (2014) 46–61.